THE JOURNAL OF COMPARATIVE NEUROLOGY 472:318–329 (2004)

Immunohistochemical Localization of Aspartoacylase in the Rat Central Nervous System

CHIKKATHUR N. MADHAVARAO,[1] JOHN R. MOFFETT,[1] ROGER A. MOORE,[2] RONALD E. VIOLA,[2] M.A. ARYAN NAMBOODIRI,[1]* AND DAVID M. JACOBOWITZ[1,3]
[1]Department of Anatomy, Physiology and Genetics, Uniformed Services University of the Health Sciences, Bethesda, Maryland 20814
[2]Department of Chemistry, University of Toledo, Toledo, Ohio 43606
[3]Laboratory of Clinical Science, National Institute of Mental Health, National Institutes of Health, Bethesda, Maryland 20892

ABSTRACT

Aspartoacylase (ASPA; EC 3.5.1.15) catalyzes deacetylation of N-acetylaspartate (NAA) to generate free acetate in the central nervous system (CNS). Mutations in the gene coding ASPA cause Canavan disease (CD), an autosomal recessive neurodegenerative disease that results in death before 10 years of age. The pathogenesis of CD remains unclear. Our working hypothesis is that deficiency in the supply of the NAA-derived acetate leads to inadequate lipid/myelin synthesis during development, resulting in CD. To explore the localization of ASPA in the CNS, we used double-label immunohistochemistry for ASPA and several cell-specific markers. A polyclonal antibody was generated in rabbit against mouse recombinant ASPA, which reacted with a single band (~37 kD) on Western blots of rat brain homogenate. ASPA colocalized throughout the brain with CC1, a marker for oligodendrocytes, with 92–98% of CC1-positive cells also reactive with the ASPA antibody. Many cells were labeled with ASPA antibodies in white matter, including cells in the corpus callosum and cerebellar white matter. Relatively fewer cells were labeled in gray matter, including cerebral cortex. No astrocytes were labeled for ASPA. Neurons were unstained in the forebrain, although small numbers of large reticular and motor neurons were faintly to moderately stained in the brainstem and spinal cord. Many ascending and descending neuronal fibers were moderately stained for ASPA in the medulla and spinal cord. Microglial-like cells showed faint to moderate staining with the ASPA antibodies throughout the brain by the avidin/biotin-peroxidase detection method, and colocalization studies with labeled lectins confirmed their identity as microglia. The predominant immunoreactivity in oligodendrocytes is consistent with the proposed role of ASPA in myelination, supporting the case for acetate supplementation as an immediate and inexpensive therapy for infants diagnosed with CD. J. Comp. Neurol. 472:318–329, 2004.

Indexing terms: ASPA; deacetylase; N-acetylaspartate; oligodendrocytes; Canavan disease; myelin deficiency; microglia; acetate

Grant sponsor: National Institutes of Health; Grant number: RO1 NS39387 (M.A.A.N.); Grant sponsor: the Samueli Institute for Information Biology; Grant number: G170ON.

Roger A. Moore's current address is Laboratory of Persistent Viral Disease, Rocky Mountain Laboratories, National Institute of Allergy and Infectious Disease, National Institutes of Health, 903 S. 4th St., Hamilton, MT 59840.

*Correspondence to: M.A. Aryan Namboodiri, Department of Anatomy, Physiology and Genetics, 4301 Jones Bridge Road, USUHS, Bethesda, MD 20814. E-mail: anamboodiri@usuhs.mil

Received 3 September 2003; Revised 11 December 2003; Accepted 16 December 2003

DOI 10.1002/cne.20080

Published online the week of March 15, 2004 in Wiley InterScience (www.interscience.wiley.com).

Aspartoacylase (ASPA; EC 3.5.1.15) catalyzes deacetylation of N-acetylaspartate (NAA), a highly abundant (~10 mM) amino acid derivative in the central nervous system (CNS), to generate free acetate in the brain (D'Adamo et al., 1972). Mutations in the gene coding ASPA cause Canavan disease (CD), an autosomal recessive neurodegenrative disorder that results in death, typically before 10 years of age (Matalon et al., 1995). The functional role of ASPA in the nervous system and the pathogenesis of CD both remain matters of controversy. We have hypothesized that 1) ASPA is actively involved in myelin synthesis by providing acetate that is used for acetyl CoA synthesis, the precursor for the subsequent synthesis of the lipid portion of myelin and 2) CD results from defective myelin synthesis caused by a deficiency in the supply of NAA/ASPA-derived acetate (D'Adamo et al., 1968; Mehta and Namboodiri, 1995; Kirmani et al., 2002, 2003). Consistent with this hypothesis it was reported from biochemical studies and in situ hybridization studies that ASPA activity is localized primarily in oligodendrocytes in the CNS (Baslow et al., 1999; Kirmani et al., 2002; Madhavarao et al., 2002) and that the developmental increase of ASPA in oligodendrocytes parallels myelination (Kirmani et al., 2003).

Although the majority of ASPA containing cells in the CNS appeared to be oligodendrocytes based on their location and morphology, it was not clear from the earlier in situ hybridization studies whether a subpopulation of some other cell type also contained ASPA. Attempts to address this issue by using double labeling with marker antibodies were not successful, because the immunohistochemistry procedure interfered with in situ hybridization. To overcome this problem, polyclonal antibodies were generated against murine recombinant ASPA for colocalization studies. The results show that ASPA is localized primarily in oligodendrocytes and is not detectable in astrocytes in the rat CNS. However, a lower level of ASPA immunoreactivity was detectable in microglia throughout the brain and in some neurons in the hindbrain. Thus, the present results corroborate the earlier in situ hybridization results, while raising interesting questions about the possible presence of ASPA in microglia and neurons.

MATERIALS AND METHODS

Purification of recombinant mouse ASPA

Purified recombinant mouse ASPA was used as antigen and was prepared as previously described (Moore et al., 2003). Briefly, the *ACY2* gene encoding murine brain aspartoacylase was amplified by polymerase chain reaction (PCR) from plasmid DNA and expressed using a pET expression system with a hexahistidine tag at the N-terminus in Rosetta Codon-Plus *Escherichia coli* cells. The enzyme was expressed primarily as inclusion bodies, but a moderate portion was obtained as soluble extract. The soluble crude extract could be kept at 4°C for 2–3 days without significant loss of activity. The enzyme was captured by anion exchange chromatography, with the eluted protein passed through a cation exchange resin (HiTrap SP; Biosciences, Piscataway, NJ) to remove additional impurities. Enzyme preparations with 90–95% purity were obtained for immunization purposes from inclusion bodies that were solubilized and refolded in either Tris or HEPES buffer, pH 7.0, in the presence of 1 mM dithiothreitol (DTT), 0.1% Triton X-100 or NP-40, 0.5 mM Zn $(OAc)_2$, and 1 mM Mg $(OAc)_2$ (cf. Moore et al., 2003).

Western blotting

ASPA immunoreactivity was tested by Western blotting against the cytosolic fraction of the rat brain homogenate (10% wt/vol) obtained by centrifugation (16,000*g*, 30 minutes) and the myelin fraction obtained by sucrose density gradient centrifugation according to the procedure of Norton and Poduslo (1973). Protein-G-purified antibodies were used at dilutions of 1:500–1:2,000. Approximately 150 μg of the crude protein were loaded from the cytosolic and myelin fractions to a precast 4–12% gradient polyacrylamide gel (Tris-glycine), and, after electrophoresis, gels were washed in distilled water for 5 minutes. Gels were blotted onto a polyvinylidine difluoride (PVDF) immobilon membrane (Sigma, St. Louis, MO) with Tris-glycine-methanol (10%) transfer buffer (Invitrogen, La Jolla, CA) for 2 hours 30 minutes at 25 V constant setting. After transfer, the membrane was washed for 5 minutes once with wash buffer [PBS-Tween 20 (0.01%), pH 7.4], and nonspecific binding sites were blocked with 5% normal goat serum (NGS) in the same buffer for 1 hour. After the blocking, the membrane was washed four times with wash buffer. The membrane was incubated with the ASPA antibody prepared in a solution consisting of 1% NGS in wash buffer and was agitated gently on a rocking shaker overnight at 4°C. After antibody treatment, the membrane was washed four times and treated for 1 hour at room temperature with a goat anti-rabbit secondary antibody (5 μg/ml) conjugated with horseradish peroxidase (HRP) prepared in the wash buffer containing 1% NGS. The blots were visualized by using diaminobenzidene as the chromogen (Sigma Fast Tablets; Sigma).

ASPA assay

Activity of ASPA was determined in the cytosolic and purified myelin fractions to corroborate the results of Western blotting. High-sensitivity radiometric assay involving thin-layer chromatography (TLC)-based product separation and phosphor image-based quantitation was followed as previously described (Madhavarao et al., 2002). Briefly, the assay was performed by using [^{14}C]NAA as the substrate (0.8 mM) employed at a specific activity of 23.5 mCi/mmol. The enzyme sources were preincubated with Tris HCl buffer (50 mM, pH 8.0) containing 0.05% nonionic detergent (IGEPAL CA-630; Sigma) for 1 hour on ice, with periodic mixing. The assay was started by adding substrate and transferring the tubes to a 37°C water bath with incubation for 1 hour. The enzyme reaction was stopped by the addition of an equal volume of ethanol containing 1 mM unlabeled L-Asp, followed by immediate vortex mixing.

Preparation of brain tissue slices

Two perfusion protocols were used for the immunohistochemical portions of this study. For fluorescence staining, three adult male Sprague-Dawley rats (200–300 g) were fixed by perfusion with 200 ml of 10% neutral buffered formalin (Fisher Scientific, Fair Lawn, NJ), and brains were postfixed for 30 minutes at room temperature. After cryoprotection with phosphate-buffered saline (PBS) containing 20% sucrose at 4°C for 2 days, the brains were frozen and 20-μm sections were cut in a cryostat and stored on chrome-alum/gelatin-coated slides at –70°C un-

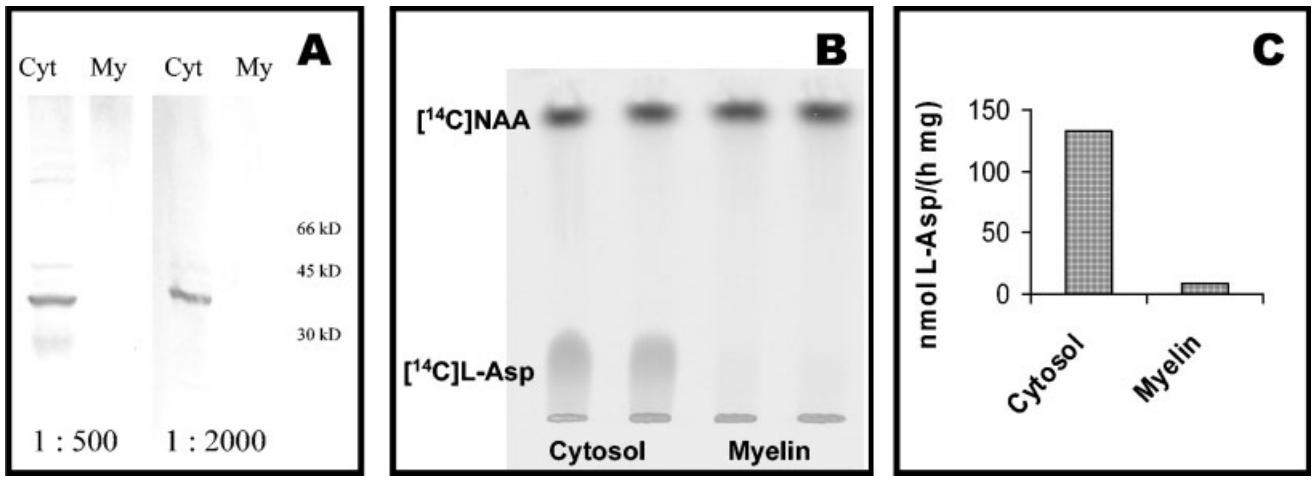

Fig. 1. Western blot (**A**), phosphor image of the TLC of enzyme assay (**B**), and ASPA activity (**C**) in the cytosol fraction and the sucrose density-purified myelin fraction from the rat brain homogenate. The rabbit ASPA antiserum was put through a protein G column and the IgG fraction collected, pooled, and used as a stock source of antibody. Antibody dilutions of 1:500–1:2,000 were adopted for the Western blotting. A prominent band corresponding to ~37 kD and several minor bands are visible in the cytosol fraction, and no band was detectable in the purified myelin fraction at a 1:500 dilution of the Ab, whereas at a 1:2,000 dilution only a single band (~37 kD) was visble in the cytosol fraction. The immunoreactivity was developed with goat anti-rabbit IgG conjugated with HRP (5 μg/ml) with diaminobenzidene chromogen after agitating the membranes for 45 minutes in a solution containing diaminobenzidene and hydrogen peroxide (Sigma Fast Tablets; Sigma). Radiometric enzyme assay for ASPA was performed, and the product was quantitated by TLC phosphor imaging as previously described (Madhavarao et al., 2002).

til further use. For avidin-biotin complex peroxidase immunohistochemistry, two animals were anesthetized with pentobarbital (200 mg/kg) and perfused transcardially with 400 ml of 10% neutral buffered formalin. Brains were removed and fixed overnight in 10% formalin before serial passage through 10%, 20%, and 30% sucrose solutions. Brains were frozen at –20°C, sectioned at a thickness of 20 μm, and stored at 4°C in PBS containing 2% NGS and 0.1% sodium azide.

Fluorescence immunohistochemistry

The protein G column-purified anti-ASPA sera were diluted 1:1,000 in PBS containing 1% NGS (or donkey serum, depending on the secondary antibody) and 0.3% Triton X-100 and were visualized with goat anti-rabbit secondary antibodies labeled with fluorescein isothiocyanate (FITC; Jackson Immunoresearch, West Grove, PA). Sections were routinely processed for indirect immunofluorescence as follows. The slides with the rat brain sections were incubated for 2 days at 0–4°C in jackets containing the primary antibodies. After incubation, the slides were washed twice for 10 minutes each in a medium containing Triton X-100 (0.2%)-PBS, pH 7.4, and incubated with the secondary antibodies for 30 minutes at room temperature. After incubation with the secondary antibodies, the slides were washed twice for 10 minutes each in medium containing Triton X-100 (0.2%)-PBS, pH 7.4, followed by washing once with PBS for 5 minutes. The slides were mounted with mounting medium [90% glycerol and 0.1% (wt/vol) p-phenylenediamine in a buffer of sodium carbonate-sodium bicarbonate, pH adjusted to 8.0] with 24- × 36-mm coverslips (20 μm thick) for analysis.

Anti-ASPA sera were used for double-fluorescence immunostaining together with monoclonal antibodies CC1 (APC; a marker for oligodendrocyte cell body; cf. Bhat et al., 1996; Dougherty et al., 2000; Tekkok and Goldberg, 2001; Ab-7; Oncogene Research Products, Cambridge, MA) at a 1:100 dilution or glial fibrillary acidic protein (GFAP; a marker for astrocytes; Boehringer-Mannheim, Indianapolis, IN) at 1:1,000 or NeuN (a marker for neurons; Chemicon International Inc., Temecula, CA) at 1:1,000, or Rip (a marker for myelin; Hybridoma Bank, University of Iowa, Ames, IA) at 1:50. The secondary antibodies were either goat anti-rabbit FITC (1:300) or donkey anti-rabbit FITC (1:100; Jackson Immunoresearch) for ASPA and goat anti-mouse Texas red (1:50) or donkey anti-mouse Texas red (1:50; Jackson Immunoresearch) for CC1, GFAP, or NeuN.

Controls for immunofluorescence were carried out by preincubating the ASPA antibody with purified ASPA antigen (5 μg/ml) overnight at 4°C and incubating the slides containing brain sections in the same jacket for 2 days at 4°C. No fluorescence signal was observed after treatment with secondary antibodies. Also, slides incubated without the primary antibodies showed no fluorescent staining when treated with secondary antibodies alone.

The issue of bleed-through was addressed by independent sections labeled for ASPA only or CC1 only, which showed true staining for anti-ASPA Ab (FITC green) or CC1 (Texas red). Furthermore, when both goat anti-rabbit FITC and goat anti-mouse Texas red were applied together to sections treated with only anti-ASPA Ab or CC1, only corresponding secondary antibodies labeled the cells. In other words, cells were labeled green only in the presence of anti-ASPA Ab and red only in the presence of CC1.

Cells positive for ASPA or CC1 and those showing both ASPA and CC1 were counted under 40× and 63× objectives on a fluorescence microscope (Leitz) equipped with both single-pass and dual-pass filter cubes. The cells positive to ASPA (FITC labeled) were counted by using a filter for green fluorescence and those positive to CC1 (Texas

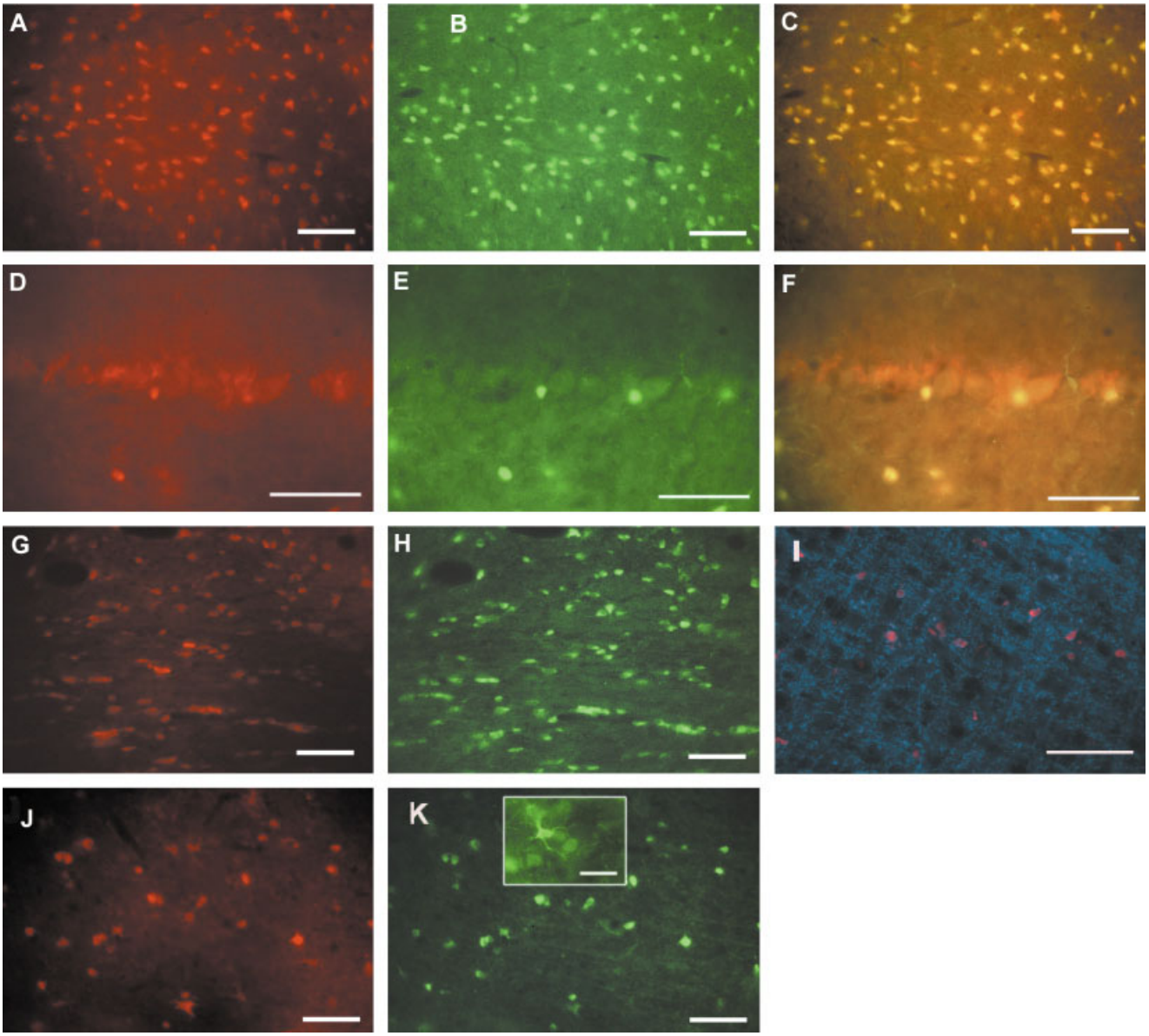

Fig. 2. Immunofluorescence labeling for CC1 (a marker for oligodendrocytes, Texas red) and ASPA (green) in sections of rat brain. The leftmost column shows CC1 (under a red filter), the middle column shows ASPA (under green filter), and the right column shows the combined images (under a dual-bandpass filter). ASPA and CC1 expression are shown in the fiber layer in the rat cerebellum (**A–C**), the Purkinje cell layer of the cerebellum (**D–F**), and the corpus callosum (**G,H**). Rip staining of myelin (AMCA, blue) and the ASPA staining of oligodendrocyte cell body (Texas red) are superimposed (**I**). Coexpression of CC1 and ASPA in layer 2 of somatosensory cortex (**J,K**). The **inset** in K at higher magnification (taken with a longer exposure) shows an ASPA-stained cell with the labeled processes. Protein G purified anti-ASPA serum (1:1,000) was used in all these studies. Scale bars = 50 μm in A–I; 30 μm in inset.

red labeled) were counted by using a filter for red fluorescence. Coexpression of proteins within individual cells was detected with a dual-bandpass filter cube, which allows both green and red fluorescence to be viewed simultaneously (excitation 480, 550 nm; emission 535, 630 nm; dichroics 505, 595 nm). Double-labeled cells appeared yellow to orange. Cells were counted in five or more nonoverlapping, independent fields under each magnification, and the numbers were expressed in percentages for comparison.

Peroxidase immunohistochemistry

For avidin-biotin complex/peroxidase immunohistochemistry, tissue sections were processed by the free-floating method. Sections were blocked against nonspecific antibody binding by incubation in PBS containing 2% normal goat serum (NGS) and 0.1% sodium azide. Endogenous peroxidase was blocked by washing sections in PBS and incubating them in a 50:50 mixture of methanol and water containing 1% H_2O_2 for 30 minutes with agitation.

TABLE 1. Number of Cells Showing ASPA (Green Fluorescence of FITC) and CC1 (Red Fluorescence of Texas Red) or Exclusively ASPA or CC1 in Cortex, Corpus Callosum and Cerebellum Areas in the Sections of Rat Brain with Use of the Common Filter[1]

Area	Number of fields	Number of cells	Cells + for red and green (%)	Cells + for green only (ASPA) (%)	Cells + for red only (CC1) (%)
Cortex	11	361	333 (92.2)	9 (2.5)	19 (5.3)
Corpus callosum	10	433	421 (97.2)	0	12 (2.8)
Cerebellum	5	408	402 (98.5)	0	6 (1.5)

[1]Cells showing red and green fluorescence appeared orange/amber under common filter; cells showing only green fluorescence or red fluorescence were verified under all three filters before considering either green (ASPA) only or red (CC1) only cells for counting purposes. Values in parenthesis show the percentage of cells from among the total number counted.

The antibody diluent solution was composed of 2% NGS in PBS with 0.1% sodium azide. Free-floating tissue sections were incubated overnight at room temperature with crude ASPA antibodies (diluted 1:5,000 to 1:10,000) in 35-mm culture dishes with constant rotary agitation. The bound antibodies were visualized by the avidin-biotin complex method with HRP as the enzyme marker (Vectastain Elite; Vector, Burlingame, CA). The sections were incubated with the biotinylated secondary antibody and avidin-peroxidase complex solutions for 80 minutes each. After final washing, the sections were developed with an Ni- and Co-enhanced diaminobenzidene chromogen (Pierce Chemical Co, Rockford, IL). Images were acquired on a Zeiss Axioplan 2 microscope and were prepared with PC-based imaging software (Adobe Systems Inc.).

Double-labeling immunohistochemistry was performed by sequential processing for the two markers, including ASPA colocalization experiments with antibodies to GFAP, a marker for astrocytes, and the lectin *Griffonia simplicifolia* isolectin B4 (GSL-IB_4), a marker for microglia. Sections were treated as described above to block endogenous peroxidase activity and nonspecific binding. ASPA antibodies were applied overnight at a dilution of 1:5,000 and were processed with the biotinylated secondary antibody and avidin-peroxidase complex as described above. The signal for the first antibody was developed with the standard diaminobenzidine chromogen system, which yields a brown/orange reaction product. The first peroxidase marker was inhibited as described above for endogenous peroxidase. The sections were then incubated for 30 minutes with 2% NGS, and then antibodies to GFAP were applied overnight with constant agitation at a dilution of 1:7,000. The sections were washed three times and then incubated for 90 minutes with 5 μg/ml of goat anti-rabbit secondary antibody labeled directly with HRP. Sections were developed for the second antigen with a purple peroxidase chromogen (VIP; Vector) and washed thoroughly. Control experiments included the omission of primary antibody and antigen-mediated blocking of the immunohistochemical signal with 500 ng/ml of the recombinant ASPA protein.

The double-labeling experiments for ASPA and lectin were also performed sequentially. ASPA immunohistochemistry was performed as described above, followed by lectin histochemistry with GSL-IB_4 labeled directly with HRP. After development of the sections for ASPA immunoreactivity as described above with diaminobenzidine as the chromogen, the sections were incubated in 50:50 methanol/water containing 1% H_2O_2 to eliminate remaining peroxidase activity. The lectin buffer was composed of 10 mM HEPES-buffered saline containing 0.1% Triton, 10 mM $CaCl_2$, 1 mM $MnCl_2$, and 1 mM $MgCl_2$. Tissue sections were soaked in lectin buffer for 15 minutes before incubating them for 90 minutes at room temperature with 20 μg/ml of GSL-IB_4–HRP in lectin buffer containing 0.5% bovine serum albumin. Sections were washed for 20 minutes in PBS before development with the purple peroxidase chromogen (VIP; Vector).

RESULTS

Polyclonal antibodies to murine recombinant ASPA raised in rabbit were found to react with a single protein band on Western blots of rat brain homogenates. Figure 1A shows a Western blot of a rat brain homogenate supernatant (cytosol fraction) and myelin purified by sucrose density centrifugation with the protein-G-purified rabbit antisera diluted 1:2,000. A single, prominent band was visible at ~37 kD, corresponding to ASPA in the brain homogenate but not with myelin. At dilutions of 1:500 or less, additional minor bands could be seen with the brain homogenate but not with myelin. Immunohistochemistry with crude antiserum showed patterns of immunoreactivity identical to those with purified antiserum, but the crude antiserum could be diluted two or three times further. The high affinity and selective immunoreactivity of these polyclonal antibodies made them suitable for immunohistochemical studies. Figure 1B shows the phosphor image of the TLC separation of the ^{14}C-labeled substrate (NAA) and product (L-Asp) of ASPA enzyme assays run on brain homogenate cytosol fraction and the sucrose density purified myelin. Myelin showed only 1/15 the activity found in brain homogenate supernatants (Fig. 1C). The ASPA activity was barely detectable in the myelin fraction, even with the highly sensitive radiometric assay (Madhavarao et al., 2002).

Double-label immunofluorescence was used to investigate expression of ASPA in different cell types in the rat CNS. Specific markers for different cell types were employed for these studies, including NeuN for neurons, GFAP for astrocytes, CC1 (Ab-7) for oligodendrocytes, and Rip for myelin. ASPA consistently colocalized with CC1, a marker antibody for oligodendrocyte cell bodies. Figure 2 shows the colocalization of ASPA and CC1 in the Purkinje cell layer and axonal fiber layer of the cerebellum, corpus callosum, and layer 2 of primary somatosensory cortex of the rat CNS. The patterns of staining for CC1 and ASPA were very similar. In white matter (Fig. 2A–C,G), both antibodies labeled rows of cell bodies lying between bundles of myelinated axons, a distribution pattern characteristic of oligodendrocytes. Small, scattered cells were labeled in both cerebellar (Fig. 2D–F) and cerebral (Fig. 2I–K) cortices. Rip stained myelin (AMCA blue) and ASPA stained oligodendrocyte cell bodies (Texas red), clearly seen in the superimposed Figure 2I. In the primary somatosensory cortex, the ASPA antibodies occasionally labeled oligodendrocyte processes (Fig. 2K, inset). No colocalization of ASPA immunoreactivity was observed in

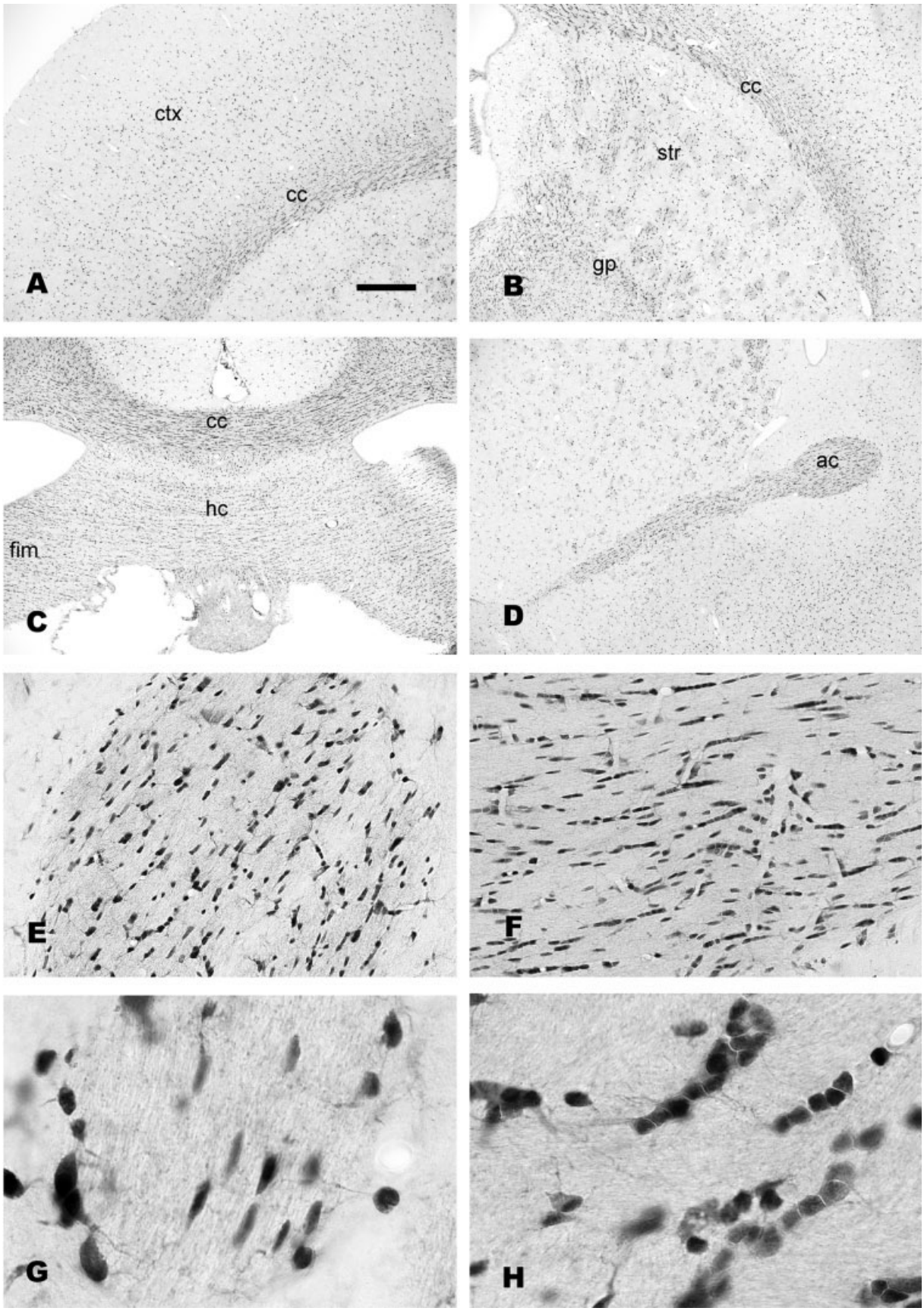

Figure 3

double-label immunofluorescence with neurons or astrocytes. Rip antibodies labeled bundles of myelin with a distinct pattern that was not seen with the ASPA antibodies (cf. Fig. 2I).

Table 1 shows the percentage of cells having both CC1 and ASPA immunoreactivity in the three regions of the rat brain used for statistical analysis. Greater than 92% of the cells showed immunostaining for both CC1 and ASPA in cerebral cortex, whereas greater than 98% were stained for both markers in the cerebellum.

The avidin/biotin complex (ABC) method of immunohistochemical detection is five to ten times more sensitive than immunofluorescence methods. This amplified detection method afforded a much more detailed staining pattern for ASPA immunoreactivity than did fluorescence detection. Specifically, the ABC method permitted visualization of fine processes emanating from oligodendrocytes in both white and gray matter as well as detection of other cell types having lower levels of immunoreactivity with the ASPA antibodies.

Oligodendrocytes were immunoreactive throughout their cell bodies, with strong immunoreactivity in the cytoplasm as well as cell nuclei. The significance of the presence of ASPA in the nuclei of oligodendrocytes is unclear. Figure 3 shows the distribution of ASPA in various parts of the rat forebrain, such as corpus callosum and cortex (Fig. 3A), striatum and internal capsule (Fig. 3B), fimbria/hippocampal commissure (Fig. 3C), and anterior commissure (Fig. 3D). ASPA-immunoreactive oligodendrocytes were present in both white and gray matter, but the density of immunoreactive cells was greater in white matter and in regions with en passant axons, such as the globus pallidus and lateral hypothalamus. In white matter, ASPA-immunoreactive oligodendrocytes were often arranged in rows between axonal bundles (Fig. 3E,F). At higher magnification, ASPA-immunoreactive cell processes could be seen on many oligodendrocytes (Fig. 3G,H). Few ASPA-immunoreactive oligodendrocytes were observed in superficial cortical layers, whereas substantial numbers of strongly stained cells were seen in deeper cortical layers.

The ABC method of immunohistochemistry showed numerous ASPA-immunoreactive oligodendrocytes throughout the thalamus, midbrain, and medulla. In the cerebellar cortex, the great majority of ASPA-immunoreactive oligodendrocytes was present in white matter, with lower numbers scattered in the granule cell and Purkinje cell layers (Fig. 4A,B). Few or no stained cells were seen in the molecular layer of the cerebellar cortex, which contains little or no myelin. In the cerebellar nuclei and arbor vitae, ASPA-immunoreactive oligodendrocytes were present in great numbers, arranged in rows between fascicles of axons (Fig. 4C). Immunoreactive oligodendrocytes were also present in the pyramids and throughout the fiber rich regions of the brainstem (Fig. 4D). The brainstem, medulla, and spinal cord exhibited an interesting pattern of immunoreactivity in which some motor and reticular neurons were stained lightly with the ASPA antibodies (Fig. 4E,H). Many ascending and descending axonal fibers in the medulla and spinal cord contained moderate levels of ASPA immunoreactivity (see Fig. 4F,H). The density of immunoreactive oligodendrocytes was exceptionally high in the white matter of the medulla (Fig. 4G) and spinal cord (data not shown).

Microglia showed faint staining with the ASPA antibodies throughout the brain, and the identity of these cells was confirmed by the double labeling with lectin (see below). In cerebral cortex, ASPA-immunoreactive microglia could be seen in all layers, but, in deeper layers, microglia were greatly outnumbered by much more intensely stained oligodendrocytes (Fig. 5A). In superficial layers of cerebral cortex, lightly stained microglia were the predominant ASPA-immunoreactive cells (Fig. 5B).

Figure 6 shows double-labeling immunohistochemistry for ASPA (orange/brown) and GFAP (a marker for astrocytes: purple in Fig. 6A,B) as well as ASPA and a lectin marker for microglia, GSL-IB_4 (purple in Fig. 6D–F). The absence of double labeling for GFAP and ASPA clearly demonstrates that astrocytes did not have detectable immunoreactivity for ASPA throughout the brain, including corpus callosum (Fig. 6A) and layers III–IV of cerebral cortex (Fig. 6B). In contrast, double-labeling experiments with ASPA antibodies and the lectin marker for microglia showed that a population of microglia was double-stained for both markers (Fig. 6C–E). However, many microglia were positive for lectin binding but negative with the ASPA antibodies (Fig. 6F).

DISCUSSION

Oligodendrocytes produce the protein and lipid components of myelin and transport them to processes, where they are used to generate the myelin sheaths surrounding neuronal axons. Although much is known about the process of axonal myelination, many details remain obscure. It has been known for some time that deficiencies in brain ASPA activity generate large increases in the concentration of NAA in the urine (Jakobs et al., 1991; Kelley and Stamas, 1992). The lack of enzyme activity results in a progressive infantile or childhood leukodystrophy that prevents proper axonal myelination in the CNS, invariably leading to death before adolescence. D'Adamo and coworkers (1966, 1968, 1972) were the first to propose that NAA-derived acetate was involved in fatty acid synthesis in the brain. In 1987, Hagenfeldt and colleagues proposed that the dysmyelination occurring in CD was due to the failure of ASPA to deacetylate NAA, preventing the transfer of acetyl groups from mitochondria to the cytosol, a process that is required for lipogenesis. Despite the fact that this hypothesis fits well with clinical and experimental findings, it does not enjoy universal acceptance among researchers in the field. More recent studies have provided

Fig. 3. Histological pattern of ASPA immunoreactivity in various regions of rat forebrain. The corpus callosum (cc) and cerebral cortex (ctx) demonstrate the difference in staining patterns for white and gray matter, with denser packing of immunoreactive cells in fiber pathways than in cortical areas (**A**). Immunoreactive oligodendrocytes were seen aligned in rows between axons of the corpus callosum and were scattered throughout cortex, being more prevalent in deeper cortical layers. Oligodendrocytes stained for ASPA were concentrated in the axon bundles of the internal capsule in the striatum (str; **B**) and were densely packed in the globus pallidus (gp). Immunoreactive oligodendrocytes were arranged in rows in the hippocampal commissure (hc), fimbria (fim; **C**), and anterior commissure (ac; **D–F**). At higher magnification, immunoreactive cell processes could be seen emerging from stained oligodendrocytes, as seen in the internal capsule (**G**), and corpus callosum (**H**). Crude anti-ASPA serum was used (1:5,000) in these studies. Scale bar = 250 μm in A (applies to A–D); 100 μm for E,F; 25 μm for G,H.

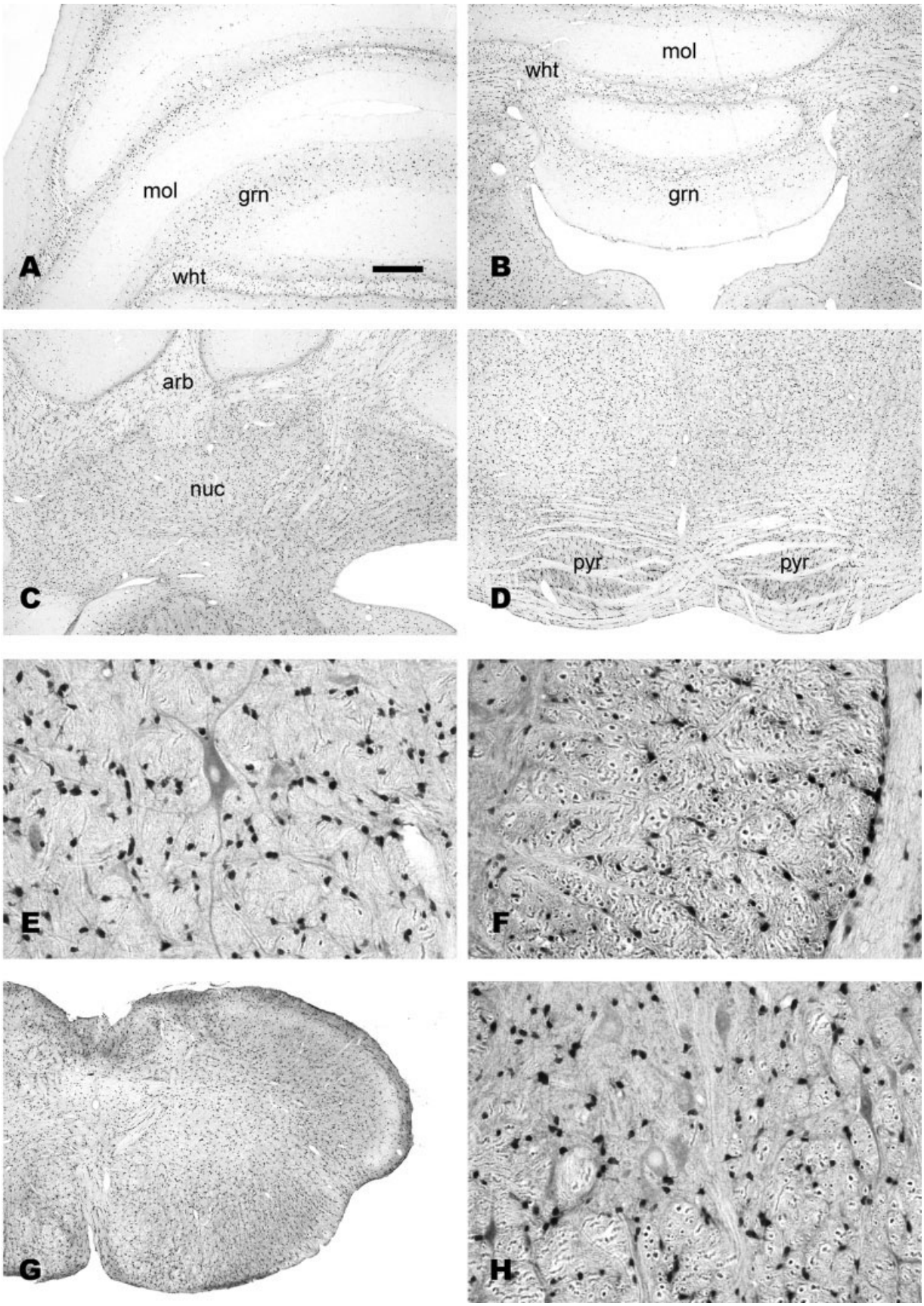

Figure 4

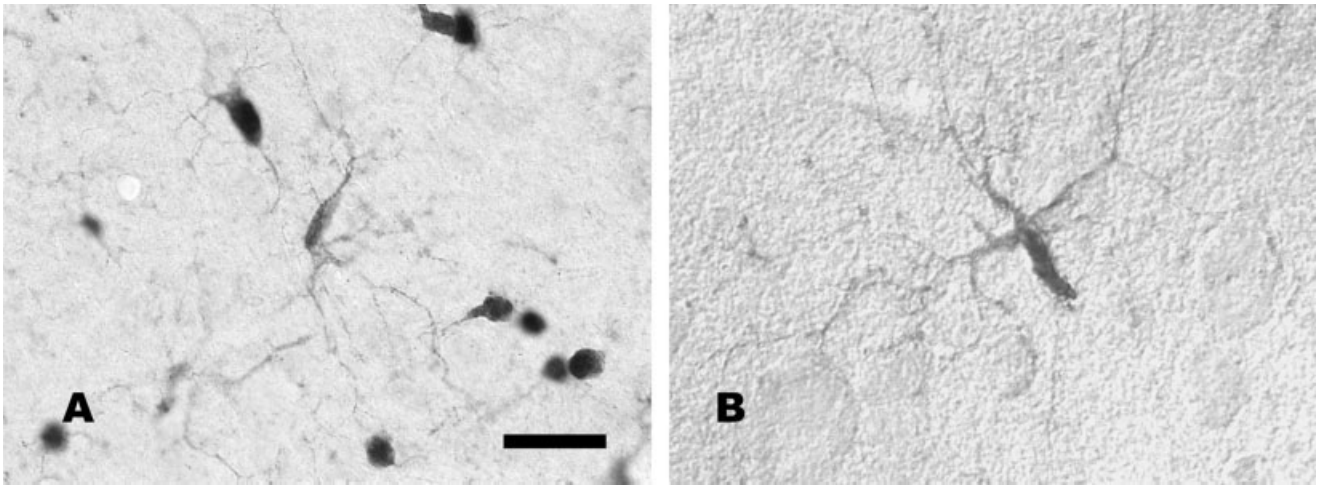

Fig. 5. Microglial cells were lightly to moderately stained for ASPA throughout the brain. In deeper layers of cerebral cortex, stained microglia were intermingled with ASPA-immunoreactive oligodendrocytes (**A**). In the superficial layers of cerebral cortex, only microglia were stained for ASPA (**B**). Crude anti-ASPA serum was used (1:5,000) in these studies. Scale bar = 40 μm in A; 50 μm for B.

direct experimental support for the hypothesis that one primary role of NAA in the CNS is as a source of acetate for the production of acetyl CoA. Mehta and Namboodiri (1995) showed incorporation of NAA-derived acetate into brain and liver lipids via acetyl CoA production. Chakraborty and coworkers (2001) demonstrated in vivo that neuronal NAA contributes to lipid synthesis in white matter, suggesting the transfer of NAA from neuron to oligodendrocyte. They also found differential incorporation of the acetate moiety from NAA, compared with free acetate, into different lipid fractions over time. Both precursors were incorporated similarly into the cholesterol and ethanolamine phosphoglyceride fractions 8 days and 33 days after radiolabeled acetate administration. However, dramatically more acetate incorporation occurred in the choline phosphoglyceride fraction from NAA at 33 days postadministration. This relatively slower turnover of NAA-derived acetate could indicate that free acetate is preferentially utilized for synthesis of choline phosphoglycerides when available, but, when free acetate levels are insufficient, ASPA-mediated release of acetate from NAA may become more important.

This study and other localization studies support the proposal that neuronal NAA is used as a source of acetate for lipid synthesis in oligodendrocytes. NAA has been shown to be present predominantly in neurons (Moffett et al., 1991; Moffett and Namboodiri, 1995), suggesting that the source of substrate for the ASPA present in oligodendrocytes is neuronal. The current investigation is the first to demonstrate directly that ASPA is localized in oligodendrocytes throughout the CNS. In our fluorescence studies, the anti-ASPA antibody colocalized with CC1, which is a known oligodendrocyte cell body marker (Bhat et al., 1996; Dougherty et al., 2000; Tekkok and Goldberg, 2001), but it did not colocalize with marker antibodies specific for neurons, astrocytes (fluorescence data not shown; Fig. 6), or myelin (Fig. 2I). Even though proximal oligodendrocyte processes were stained for ASPA, the staining pattern for Rip in myelin bundles was not observed with the ASPA antibodies (Fig. 2I). Moreover, myelin purified by standard sucrose density centrifugation did not show a 37-kD band on Western blots of rat brain homogenate supernatants, which is similar to observations described in a recent report by another group (Klugmann et al., 2003). The purified myelin fraction showed little or no ASPA enzymatic activity compared with the brain homogenate supernatant, as measured by using a highly sensitive radiometric assay (cf. Madhavarao et al., 2002). The report by Klugmann et al. (2003) showed another band of ~85 kD in addition to the ~37-kD band in their rat brain homogenates with their polyclonal anti-ASPA antibody. We have not detected this ~85-kD band in immunoblots with SDS-PAGE. Occurrence of aggregates in recombinant proteins expressed in bacterial cells is not uncommon (cf. Darby and Creighton, 1995; Stempfer et al., 1996), whereas native mammalian ASPA, even if it occurs as a homodimer in vivo should be converted to monomers under reducing SDS-PAGE conditions, unless the two monomers are covalently attached. We did not see an ASPA dimer equiv-

Fig. 4. ASPA immunoreactivity in cerebellum, brainstem, and spinal cord. Oligodendrocytes were densely packed in rows in the cerebellar white matter (wht) but were thinly distributed in the granule cell (grn) and Purkinje cell layers (**A,B**). Only scattered stained cells were observed in the cerebellar molecular layer (mol), and most of these were lightly stained cells with the morphology of microglia. Immunoreactive oligodendrocytes were densely packed in the cerebellar nuclei (nuc) and arbor vitae (arb; **C**) and were similarly concentrated in the pyramids (pyr) and adjacent brainstem (**D**). In the brainstem, some neurons were moderately immunoreactive for ASPA, and many ascending axons contained moderate to strong ASPA immunoreactivity. A large ASPA-immunoreactive neuron of the pontine reticular nucleus is shown here surrounded by oligodendrocytes and stained axons (**E**). Axons stained for ASPA in the spinal trigeminal tract are shown cut in cross-section, with the myelin sheaths unstained (**F**). **G** shows the staining pattern for ASPA in the medulla, and **H** shows ASPA staining in the ventral horn of the spinal cord. Crude anti-ASPA serum was used (1:5,000) in these studies. Scale bar = 240 μm in A (applies to A–D); 80 μm for E,F,H; 450 μm for G.

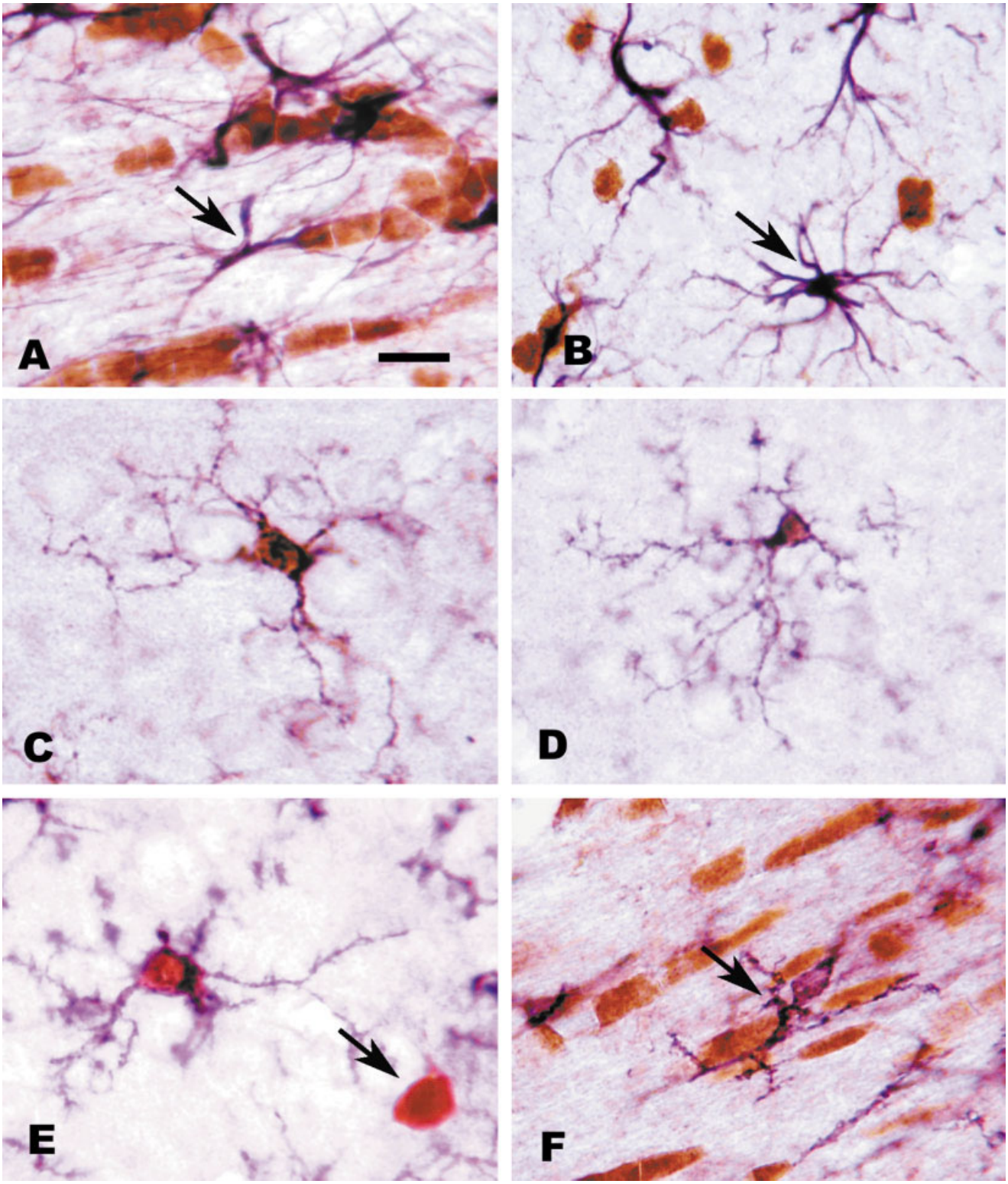

Fig. 6. Double-labeling experiments for ASPA with GFAP and GSL-IB_4. Double labeling experiments for ASPA and the astrocyte marker GFAP demonstrated that these proteins were present in distinct cell populations throughout the brain. In the corpus callosum, oligodendrocytes (orange/brown) and astrocytes (purple, arrow) were both present in large numbers but were distinctly labeled for only one of the two markers (**A**). The same segregation of immunoreactivity patterns was observed in deeper layers of the cerebral cortex, ASPA immunoreactivity (orange/brown) being associated with oligodendrocytes and GFAP staining (purple, arrow) occurring only in astrocytes (**B**). Colocalization studies with ASPA antibodies and GSL-IB_4, a lectin that labels microglia and endothelia, showed that these two markers were colocalized in microglial cells throughout the brain. Microglia were typically lightly to moderately stained for ASPA (orange/brown) while also expressing lectin-binding carbohydrates on their cell bodies and processes (purple; **C,D**). A double-labeled microglial cell is shown from layers II–III of cerebral cortex, where a nearby oligodentrocyte is seen labeled for ASPA only (arrow in **E**). Many lectin-stained microglia were not stained for ASPA, as in the case of this microglial cell in the corpus callosum (arrow in **F**), surrounded by ASPA-IR oligodendrocytes (orange/brown). Crude anti-ASPA serum was used (1:5,000) in these studies. Scale bar = 20 μm in A (applies to A,C,E,F); 30 μm for B,D.

alent band with our polyclonal antibody in Western blots by SDS-PAGE (Fig. 1).

Between 92% and 98% of the cells positive for CC1 also showed ASPA immunoreactivity, depending on the neuroanatomical location. Oligodendrocytes labeled for ASPA displayed distinct morphologies in gray and white matter. In gray matter areas, multiple proximal cell processes were often seen on individual stained cells (Fig. 1K, inset), whereas, in fiber-rich white matter regions, immunoreactive cells were compact and arranged in rows with one or no visible processes.

In the present investigation, the ABC method for detecting ASPA in the rat brain provided a substantially more detailed pattern of staining for oligodendrocytes than the fluorescence method. Additionally, the ABC method revealed low levels of immunoreactivity in cell types other than oligodendrocytes. In rat forebrain, little or no ASPA immunoreactivity was observed in neurons, but, in hindbrain, small populations of lightly stained neurons were observed, especially some reticular and motor neurons of the medulla and spinal cord. In addition, many ascending and descending spinal and medullary axons were moderately immunoreactive with the antibodies to ASPA. The exact nature of ASPA immunoreactivity of neurons and axons with the current ASPA antibodies in brainstem and spinal cord axons remains to be determined. A new protein has been recently added to the NCBI database that has a significant degree of sequence homology with ASPA (accession No. Q96HD9), and it is possible that the polyclonal antibodies stain this protein or other proteins with sequence homology to ASPA. Ultrastructural immunocytochemical methods will be useful for delineating the nature of axonal staining. It is also possible that ASPA is expressed at lower levels in some neurons and their axons. If so, the roles that might be served by ASPA in neurons are unknown, but possibilities include enzyme-mediated liberation of aspartate for use as a neurotransmitter and/or to provide substrate (via formation of acetyl CoA) for various neuronal acetylation reactions. However, the predominant localization of ASPA in oligodendrocytes and the presence of NAA primarily in neurons suggest that neurons transfer intact NAA to oligodendrocytes, wherein ASPA cleaves the acetate moiety, which can then be used for lipogenesis related to myelination.

A surprising finding in the present study was the presence of mild ASPA immunoreactivity in the cytoplasm and nuclei of microglia in all regions of the brain. In earlier studies that used in situ hybridization, no signal was detectable in microglia (Kirmani et al., 2002, 2003). This might reflect the lower level of sensitivity of the in situ hybridization technique used in those studies. Conversely, it is also possible that microglia contain a protein with some sequence similarity to ASPA that is recongnized with lower affinity by the antibodies produced in this study. The microglia with low-level immunoreactivity were ramified in morphology, typical of resting microglia.

The detection of ASPA immunoreactivity in the nuclei of oligodendrocytes and microglia raises the possibility that ASPA may not be restricted to a single function. In a scenario in which more than one function is attributable to ASPA, a therapeutic strategy for CD based on acetate supplementation may prove insufficient to deal with all of the resultant metabolic deficiencies. Studies are underway in our laboratory to determine the nature of ASPA immunoreactivity in microglia in response to various immune-activating agents, such as lipopolysaccharide, which could indicate some additional role for ASPA or an ASPA-like protein in the immune response.

The acetate deficiency hypothesis of CD and the concept of acetate supplementation therapy, which we have proposed previously (Kirmani et al., 2002), deserve some discussion. Several lines of evidence strongly implicate NAA in brain lipid metabolism via acetate liberation and argue in favor of acetate supplementation as a possible treatment for CD. First, studies have shown that free acetate is almost as effective as the acetyl moiety of NAA for fatty acid/lipid synthesis in the nervous system during myelination (D'Adamo and Yatsu, 1966; D'Adamo et al., 1968; Burri et al., 1991). Recently, it has been demonstrated that intraneuronal NAA does supply acetyl groups for myelin lipid synthesis in oligodendrocytes (Chakraborty et al., 2001). Second, in the developing rat, as much as 10% of the radiolabeled acetate administered intraperitoneally is incorporated into brain lipids, whereas only about 5% is incorporated into lipids in the liver (Dhopeshwarker and Mead, 1973), indicating that acetate delivered systemically contributes robustly to myelination. Third, the relatively high K_m (3–4 mM) of the uptake system for acetate across the blood–brain barrier would permit increased uptake of acetate into brain when blood levels are increased (Terasaki et al., 1991). Finally, significant neurological improvement was observed when calcium acetate was administered to a CD patient to manage hyperphosphatemia (Leone et al., 1999). The results in the present study favor the use of dietary acetate supplementation as a possible therapeutic approach to prevent the development of CD leukodystrophy.

LITERATURE CITED

Baslow MH, Sucknow RF, Sapirstein V, Hungund BL. 1999. Expression of aspartoacylase in cultured rat macroglial cells is limited to oligodendrocytes. J Mol Neurosci 13:47–53.

Bhat RV, Axt KJ, Fosnaugh JS, Smith KJ, Johnson KA, Hill DE, Kinzler KW, Baraban JM. 1996. Expression of the APC tumor suppressor protein in oligodendroglia. Glia 17:169–174.

Burri B, Steffen C, Herschkowitz N. 1991. N-acetylaspartate is a major source of acetyl groups for lipid synthesis during rat brain development. Dev Neurosci 13:403–411.

Chakraborty G, Mekala P, Yahya D, Wu G, Ledeen RW. 2001. Intraneuronal N-acetylaspartate supplies acetyl groups for myelin lipid synthesis: evidence for myelin-associated aspartoacylase. J Neurochem 78:736–745.

D'Adamo AF Jr, Yatsu FM. 1966. Acetate metabolism in the nervous system:N-acetylaspartic acid and the biosynthesis of brain lipids. J Neurochem 13:961–965.

D'Adamo AF Jr, Gidez LI, Yatsu FM. 1968. Acetyl transport mechanisms: involvement of N-acetyl aspartate in de novo fatty acid biosynthesis in the developing brain. Exp Brain Res 5:267–273.

D'Adamo AF Jr, Smith J, Woiler C. 1972. The occurrence of N-acetylaspartate amidohydrolase (aminoacylase 11) in the developing rat brain. J Neurochem 20:1275–1278.

Darby N, Creighton TE. 1995. In: Shirley BA, editor. Disulfide bonds in protein folding and stability. Protein stability and folding: theory and practice. Totowa, NJ: Humana Press, Inc.

Dhopeshwarker GA, Mead JF. 1973. Uptake and transport of fatty acids into the brain and the role of the blood–brain barrier system. Adv Lipid Res 11:109–142.

Dougherty KD, Dreyfus CF, Black IB. 2000. Brain-derived neurotrophic factor in astrocytes, oligodendrocytes, and microglia/macrophages after spinal cord injury. Neurobiol Dis 7:574–585.

Hagenfeldt L, Bollgren I, Venizelos NJ. 1987. N-acetylaspartic aciduria due to aspartoacylase deficiency—a new aetiology of childhood leukodystrophy. J Inherit Metab Dis 10:135–141.

Jakobs C, Brink HJT, Langelaar SA, Zee T, Stellaard F, Macek M, Srsnova K, Srsen S, Kleijer WJ. 1991. Stable isotope dilution analysis of N-acetylaspartic acid in CSF, blood, urine and amniotic fluid; accurate postnatal diagnosis and the potential for prenatal diagnosis of Canavan disease. J Inherit Metab Dis 14:653–660.

Kelley RI, Stamas JN. 1992. Quantitation of N-acetylaspartic acid in urine by isotope dilution gas chromatography-mass spectrometry. J Inherit Metab Dis 15:97–104.

Kirmani BF, Jacobowitz DM, Kallarakal A, Namboodiri MAA. 2002. Aspartocylase is restricted primarily to myelin synthesizing cells in the CNS: therapeutic implications for Canavan disease. Brain Res Mol Brain Res 107:176–182.

Kirmani BF, Jacobowitz DM, Namboodiri MAA. 2003. Developmental increase of aspartoacylase in oligodendrocytes parallels CNS myelination. Brain Res Dev Brain Res 140:105–115.

Klugmann M, Symes CW, Klaussner BK, Leichtlein CB, Serikawa T, Young D, During MJ. 2003. Identification and distribution of aspartoacylase in the postnatal rat brain. Neuroreport 14:1837–1840.

Leone P, Janson CG, McPhee SJ, During MJ. 1999. Global CNS gene transfer for a childhood neurogenetic enzyme deficiency: Canavan disease. Curr Opin Mol Ther 1:487–492.

Madhavarao CN, Hammer JA, Quarles RH, Namboodiri MAA. 2002. A radiometric assay for aspartoacylase activity in cultured oligodendrocytes. Anal Biochem 308:314–319.

Matalon R, Michals K, Kaul R. 1995. Canavan disease: from spongy degeneration to molecular analysis. J Pediatr 127:511–517.

Mehta V, Namboodiri MAA. 1995. N-acetylaspartate as an acetyl source in the nervous system. Brain Res Mol Brain Res 31:151–157.

Moffett JR, Namboodiri MA. 1995. Differential distribution of N-acetylaspartylglutamate and N-acetylaspartate immunoreactivities in rat forebrain. J Neurocytol 24:409–433.

Moffett JR, Namboodiri MA, Cangro CB, Neale JH. 1991. Immunohistochemical localization of N-acetylaspartate in rat brain. Neuroreport 2:131–134.

Moore RA, Le Coq J, Faehnle CR, Viola RE. 2003. Purification and preliminary characterization of brain aspartoacylase. Arch Biochem Biophys 413:1–8.

Norton WT, Poduslo SE. 1973. Myelination in rat brain: method of myelin isolation. J Neurochem 21:749–757.

Stempfer G, Holl-Neugebauer B, Rudolph R. 1996. Improved refolding of an immobilized fusion protein. Nat Biotech 14:329–334.

Tekkok SB, Goldberg MP. 2001. Ampa/kainate receptor activation mediates hypoxic oligodendrocyte death and axonal injury in cerebral white matter. J Neurosci 21:4237–4248.

Terasaki T, Takakuwa S, Moritani S, Tsuji A. 1991. Transport of monocarboxylic acids at the blood–brain barrier: studies with monolayers of primary cultured bovine brain capillary endothelial cells. J Pharmacol Exp Ther 258:932–937.